Pramana – J. Phys. (2019) 93:70
https://doi.org/10.1007/s12043-019-1827-y

A chaotic study on Heisenberg ferromagnetic spin chain using Dzyaloshinski–Moriya interactions

B S GNANA BLESSY[1,2] and M M LATHA[1,2,*]

[1]Department of Physics, Women's Christian College, Nagercoil 629 001, India
[2]Manonmaniam Sundaranar University, Abishekapatti, Tirunelveli 627 012, India
*Corresponding author. E-mail: lathaisaac@yahoo.com

MS received 6 August 2018; revised 21 March 2019; accepted 2 May 2019

Abstract. The chaotic dynamics of a one-dimensional Heisenberg ferromagnetic spin chain incorporating Dzyaloshinski–Moriya (D–M) interaction, dipole–dipole and quadrupole–quadrupole interactions has been investigated. The studies are carried out by plotting phase diagrams and chaotic trajectories. We then analyse the stability of the system using the Lyapunov stability analysis.

Keywords. Heisenberg; ferromagnetism; chaos; Dzyaloshinski–Moriya interaction.

PACS Nos 05.45.–a; 12.38.Bx; 02.30.Jr

1. Introduction

In the physical world, the property that is ubiquitous is the nonlinearity factor. Under linear approximations, nonlinear systems have been widely studied for a long time. In the 1970s, there is an explosive growth in its study. It deals with the characterisation of regular as well as chaotic motions [1]. The solutions derived from the nonlinear partial differential equations are the solitons and the solutions that are obtained from the nonlinear differential or difference equations with floating frequency and amplitude are named as chaotic motion. This motion is sensitive to the changes in initial conditions [2]. Due to vast potential applications, the studies on solitons are the main focus in the research field [3]. Ferromagnetism is one of the most important property in magnetism. Here the spins of all atoms in the ground state are oriented in one direction. This parallel alignment of spins happened due to an interaction proposed by Heisenberg which is called the exchange interaction.

In recent years, there has been a considerable interest in the study of ferromagnetic system with dipole–dipole and quadrupole–quadrupole interactions [4–11]. For soliton-like excitations in a spin chain with the quadrupole–quadrupole interaction, a study was done by Shi *et al* [12]. The coexistence of soliton and chaos in certain systems was recently proved by Kumar and Khare [13] for a range of parameter values. Motivated by this, in our previous paper [14], we have done a brief study on the chaotic behaviour of a ferromagnetic system with bilinear and biquadratic interactions. But the notable one among various types of magnetic interactions is the Dzyaloshinski–Moriya (D–M) interaction [15–17] which is an antisymmetric exchange interaction between two neighbouring magnetic spins with the total contribution of magnetic exchange interactions. With the property of linearity, explaining soliton dynamics of the ferromagnetic spin chain with the D–M interaction, a few studies have been reported in [18–21]. Many researchers have intensively investigated one-dimensional antiferromagnetism in nonlinear soliton excitations with the D–M interaction. In the absence of D–M interaction too, some studies have been conducted recently [22–29]. But so far, the studies related to chaotic dynamics in the ferromagnetic system with D–M interaction have not yet been reported. Hence, in this study, we construct a model Hamiltonian for the ferromagnetic system with D–M interaction in addition to the dipole–dipole, anisotropic and quadrupole–quadrupole interactions. The studies are further carried out by the Holstein–Primakoff (H–P) bosonic representation of spin operators followed by the perturbation technique.

The plan of this paper is as follows: Section 2 explains the formulation of the Hamiltonian for a ferromagnetic system in the quantised form by taking into account the dipole–dipole, D–M and anisotropic interactions. Hamilton's equations of motion are then used

Published online: 07 August 2019

to derive the time evolution of the system. To study the chaoticity of the ferromagnetic system, trajectories and phase-space plots are drawn. Stability is then analysed using the Lyapunov plots. In §3, we extend the same study for the ferromagnetic system with the quadrupole–quadrupole interaction. Finally, the conclusion is addressed in §4.

2. Model Hamiltonian with dipole–dipole and D–M interactions

We consider a ferromagnetic spin chain and the spin Hamiltonian for this system is written as

$$H = -\sum_i [\tilde{J}(\vec{S}_i \cdot \vec{S}_{i+1}) + \tilde{D}\vec{Z} \cdot (\vec{S}_i \times \vec{S}_{i+1}) - \tilde{A}(S_i^z)^2]. \quad (1)$$

In Hamiltonian (1), A is the anisotropic parameter which corresponds to the uniaxial crystal field anisotropy, J is the constant coefficient of bilinear exchange interaction, $\vec{S}_i = (S_i^x, S_i^y, S_i^z)$ is the spin operator at the lattice site i and D is the D–M interaction parameter between two neighbouring magnetic spins. The weak anisotropic axis corresponds to the D–M interaction and the axis of magnetisation is chosen along the z-direction. In D–M interaction, unlike the exchange and crystal field anisotropic interactions, the normal component of the nearest neighbours interacts with a component of the spin at a given lattice site i. For an anisotropic ferromagnetic spin system with the D–M interaction, the Hesienberg model of the Hamiltonian in the dimensionless form [30,31] is written as

$$H = -\sum_i \left[\frac{J}{2S^2}(\hat{S}_i^+ \hat{S}_{i+1}^- + \hat{S}_i^- \hat{S}_{i+1}^+ + 2\,\hat{S}_i^z \hat{S}_{i+1}^z) + \frac{D}{2\,i\,S^2}(-\hat{S}_i^+ \hat{S}_{i+1}^- + \hat{S}_i^- \hat{S}_{i+1}^+) - \frac{A}{S^2}(\hat{S}_i^z)^2\right]. \quad (2)$$

Using the classical approximation, for many of the ferromagnetic spin systems, the spin dynamics can be studied successfully but, for certain ferromagnetic systems, the semiclassical approach is more suitable. In the case of the semiclassical limit, to study the spin dynamics of a one-dimensional ferromagnetic spin system, the Hamiltonian has to be bosonised using the H–P representation [32] of spin operators. In the following subsection, the bosonisation for a semiclassical limit of ferromagnetic spin system is discussed.

2.1 *Semiclassical approach*

The general form of H–P approximation is written as

Table 1. Fixed points.

S. No.	x	p_x
(i)	−0.036796	0.0135895
(ii)	−0.000276241	0.0000336649
(iii)	0.0381591	−0.0120476

$$\hat{S}_n^+ = \sqrt{2}\,S\left(1 - \frac{\epsilon^2}{4}a_n^\dagger a_n\right)\epsilon a_n,$$
$$\hat{S}_n^- = \sqrt{2}\,S\epsilon a_n^\dagger\left(1 - \frac{\epsilon^2}{4}a_n^\dagger a_n\right),$$
$$\hat{S}_n^z = S - a_n^\dagger a_n. \quad (3)$$

Using the above relations in eq. (2), we get

$$\begin{aligned} H = -\Big[& A - J - \frac{1}{S}(2\,A a_n a_n^\dagger - J a_n a_n^\dagger \\ & - J a_{n+1} a_{n+1}^\dagger) + \frac{1}{S^2}(A a_n^2 a_n^{\dagger 2} - J a_n a_{n+1} a_n^\dagger a_{n+1}^\dagger) \\ & + \epsilon^2(D a_{n+1} a_n^\dagger - J a_{n+1} a_n^\dagger - D a_n a_{n+1}^\dagger - J a_n a_{n+1}^\dagger) \\ & - \frac{\epsilon^4}{4}(D a_n a_{n+1} a_n^{\dagger 2} - J a_n a_{n+1}(a_n^\dagger)^2 - D a_n^2 a_n^\dagger a_{n+1}^\dagger \\ & - J(a_n)^2 a_n^\dagger a_{n+1}^\dagger + D a_{n+1}^2 a_n^\dagger a_{n+1}^\dagger + J a_{n+1}^2 a_n^\dagger a_{n+1}^\dagger \\ & - D a_n a_{n+1} a_{n+1}^{\dagger 2} - J a_n a_{n+1}(a_{n+1}^\dagger)^2) \\ & + \frac{\epsilon^6}{16}(D a_n a_{n+1}^2 a_n^{\dagger 2} a_{n+1}^\dagger - J a_n a_{n+1}^2 (a_n^\dagger)^2 a_{n+1}^\dagger \\ & - D a_n^2 a_{n+1} a_n^\dagger a_{n+1}^{\dagger 2} - J a_n^2 a_{n+1} a_n^\dagger (a_{n+1}^\dagger)^2)\Big]. \end{aligned} \quad (4)$$

To study the chaotic dynamics of this system, we rewrite the boson operators $a_n^\dagger$ and a_n in the first quantised form. The relations we used are

$$a_n^\dagger = \left(\frac{M\omega}{2\hbar}\right)^{1/2} x - i\left(\frac{1}{2\,M\hbar\omega}\right)^{1/2} p_x,$$
$$a_n = \left(\frac{M\omega}{2\hbar}\right)^{1/2} x + i\left(\frac{1}{2\,M\hbar\omega}\right)^{1/2} p_x,$$
$$a_{n+1}^\dagger = \left(\frac{M\omega}{2\hbar}\right)^{1/2} (x+h) - i\left(\frac{1}{2\,M\hbar\omega}\right)^{1/2} p_x,$$
$$a_{n+1} = \left(\frac{M\omega}{2\hbar}\right)^{1/2} (x+h) + i\left(\frac{1}{2\,M\hbar\omega}\right)^{1/2} p_x. \quad (5)$$

In eq. (5), h is the successive distance between two unit cells, x is the exciton displacement, p_x is the exciton momentum, M is the mass of a single molecule and ω is the angular velocity. Using eq. (5) in eq. (4), we get

$$H = -\Big[A - J + \frac{1}{S}\big(h^2 J a^2 + 2\,hJxa^2 - 2\,Ax^2a^2 + 2\,Jx^2a^2 + 2\,Ap_x^2\,b^2 - 2\,Jp_x^2\,b^2\big) - \frac{1}{S^2}\big(h^2 Jx^2a^4 - 2\,hJx^3a^4 + Ax^4a^4 - Jx^4a^4 + h^2 Jp_x^2\,a^2\,b^2 + 2\,hJp_x^2\,xa^2\,b^2 - 2Ap_x^2\,x^2\,a^2b^2 + 2Jp_x^2\,x^2\,a^2\,b^2 + Ap_x^4\,b^4 - Jp_x^4\,b^4\big) - \epsilon^2\big(2\,hJxa^2 + 2Jx^2a^2 - 2Dhp_xab + 2Jp_x^2\,b^2\big)\Big]. \tag{6}$$

2.2 *Hamilton's equations of motion*

The time evolution of this ferromagnetic spin system is computed by Hamilton's equations given by

$$\frac{\mathrm{d}x}{\mathrm{d}t} = \frac{\partial H}{\partial p_x}, \tag{7}$$

$$\frac{\mathrm{d}p_x}{\mathrm{d}t} = -\frac{\partial H}{\partial x}. \tag{8}$$

Using eq. (6) in eqs (7) and (8), we get

$$\frac{\mathrm{d}x}{\mathrm{d}t} = \frac{1}{S}(4Ap_xb^2 - 4\,Jp_xb^2) + \frac{1}{S^2}(2\,h^2Jp_xa^2\,b^2 + 4hJp_xxa^2b^2 - 4Ap_xx^2\,a^2\,b^2 + 4Jp_xx^2\,a^2\,b^2 + 4Ap_x^3\,b^4 - 4Jp_x^3\,b^4) + \epsilon^2(2Dhab - 4Jp_xb^2), \tag{9}$$

$$\frac{\mathrm{d}p_x}{\mathrm{d}t} = -\frac{1}{S}(2hJa^2 - 4Axa^2 + 4Jxa^2) + \frac{1}{S^2}(2h^2Jxa^4 + 6hJx^2a^4 - 4Ax^3a^4 + 4Jx^3a^4 - 2hJp_x^2\,a^2\,b^2 + 4Ap_x^2\,xa^2b^2 - 4Jp_x^2\,xa^2b^2) + \epsilon^2(2\,hJa^2 - 4Jxa^2). \tag{10}$$

2.3 *Phase plots and irregular trajectories*

A periodic point with period equal to one is a fixed point. Equations (9) and (10) are solved using MATHEMATICA and the fixed points are calculated. They are presented in table 1. For the perturbation analysis we took the third set of values from the table. They are $x = 0.0381591$ and $p_x = -0.0120476$.

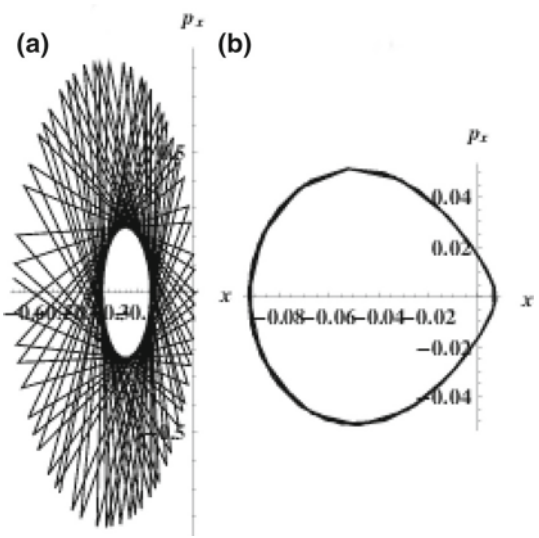

Figure 1. Phase-space plots: **(a)** unperturbed plot and **(b)** perturbed plot for $A = 0.2$, $D = 0.001$, $J = 12$, $S = 0.5$, $\epsilon = 0.5$, $x = 0.0381591$, $p_x = -0.0120476$.

In continuation with the calculation of fixed points, phase-space portraits are drawn. The phase-space plot for the unperturbed system is given in figure 1a and with added perturbation in figure 1b for $D = 0.001$. It is found that for the ferromagnetic system with the unperturbed case, the plot exhibits a complete shift to the negative scale having a densely filled region of periodic waves colliding with each other which is observed as an elliptical orbit. When perturbation is applied, the phase-space plot depicted in figure 1b is a short pyriform-shaped orbit having a slight extension towards the positive scale. It has a thick layer of chaotic cross-well patterns which appears due to the number of oscillations that slide over. The trajectories shown in figures 2a and 2b are the time series evolution plot for the unperturbed and the perturbed system, respectively. The unperturbed time series plot progresses periodically with non-sticky trajectories and figure 2b has sticky trajectories. They both exhibit a modulation in its frequency.

2.4 *Lyapunov stability*

Lypunov stability analysis plays a major role in determining the stability of the system. This analysis is sufficient to identify whether the stability of the system is periodic or chaotic. Here we study the maximal Lyapunov exponent (MLE) for two cases: (i) displacement perturbation and (ii) momentum perturbation.

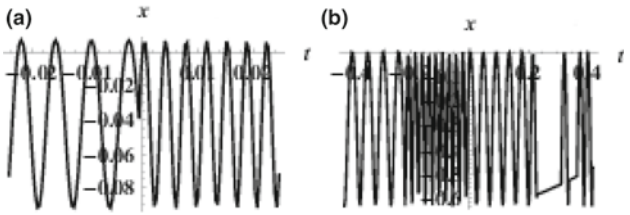

Figure 2. Trajectory plots: **(a)** unperturbed plot and **(b)** perturbed plot for $A = 0.2$, $D = 0.001$, $J = 12$, $S = 0.5$, $\epsilon = 0.5$, $x = 0.0381591$, $p_x = -0.0120476$.

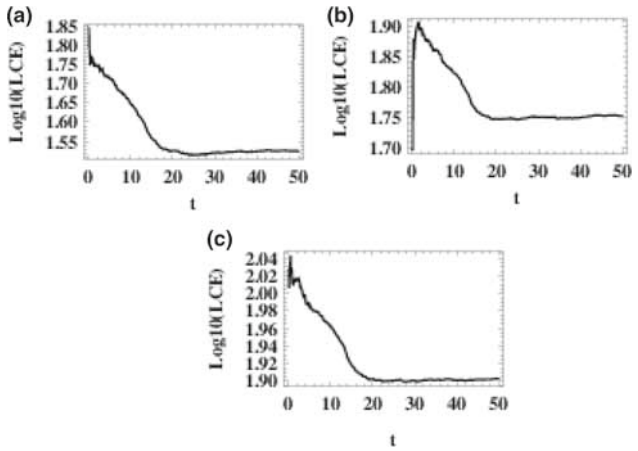

Figure 3. Lyapunov curves in terms of displacement perturbation for $A = 0.2$, $D = 0.001$, $J = 12$, $S = 0.5$, $\epsilon = 0.5$ at **(a)** 10^{-14}, **(b)** 10^{-15} and **(c)** 10^{-16}.

Table 2. MLE for different displacement perturbations.

S. No.	Size of perturbation	MLE
(a)	10^{-14}	-1.85
(b)	10^{-15}	1.91
(c)	10^{-16}	2.045

Case (i) *Displacement perturbation*: The perturbation in displacement varies from 10^{-14} to 10^{-16}. The obtained plots reveal its chaotic behaviour. Also, we perceive that the Lyapunov exponent value increases substantially as the size of perturbation increases (see figure 3). Here the MLEs are positive for more than one perturbation and so this system is considered as hyperchaotic. Table 2 gives the values for different orders of displacement perturbation.

Case (ii) *Momentum perturbation*: Figure 4 presents the Lyapunov characteristic exponent spectra for the momentum perturbation. The size of perturbation corresponding to this case are (a) 10^{-14}, (b) 10^{-15}, (c) 10^{-16}. After examining the graphs, we observe that as the size of perturbation varies, all the MLE

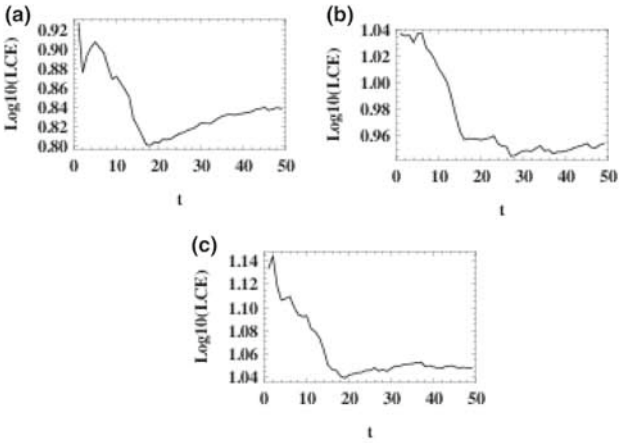

Figure 4. Lyapunov curves in terms of momentum perturbation for $A = 0.2$, $D = 0.001$, $J = 12$, $S = 0.5$, $\epsilon = 0.5$ at **(a)** 10^{-14}, **(b)** 10^{-15} and **(c)** 10^{-16}.

Table 3. MLE for different momentum perturbations.

S. No.	Size of perturbation	MLE
(a)	10^{-14}	0.92
(b)	10^{-15}	1.04
(c)	10^{-16}	1.14

values go positive. Usually, a positive MLE indicates the system to be chaotic. Table 3 contains the MLE values for different sizes of perturbation.

2.5 *Influence of D–M interaction*

The analysis is done for two sets of values: $D = 0.005$ and 0.007.

Case (i) $D = 0.005$: The phase-space portraits observed are given in figures 5 and 6. In the unperturbed system, the phase trajectory obtained discloses a star-like gesture in an elliptical orbit. The gesture has accurate fine lines crossing over in all directions. Under the perturbation technique, by adding suitable values of $x = 0.0381591$ and $p_x = -0.0120476$, the chaotic oscillations covering the edge of the pyriform-shaped orbit gets split in a different amplitude range. The time series plot obtained for the unperturbed case (figure 6a) oscillates periodically. It has non-sticky trajectories. The perturbed plot (figure 6b) resembles sticky trajectories with more decaying in its amplitude. Both the trajectories behave as a harmonic oscillator. Moving on to the detailed study on the stability of the system, the Lyapunov curves symbolify hyperchaoticity. Figures 7 and 8 display the effect of perturbation in displacement and momentum.

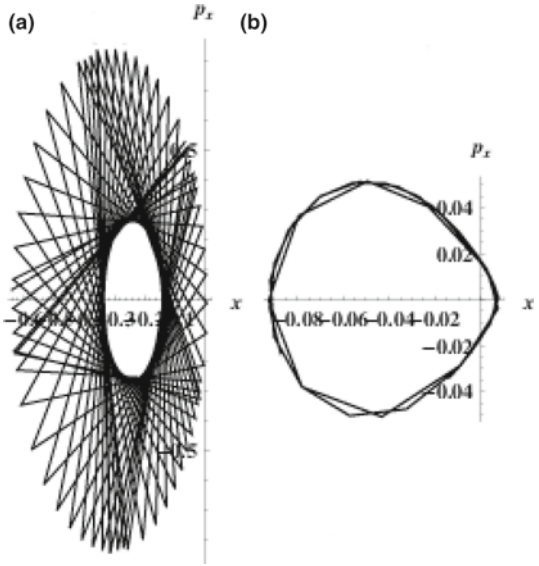

Figure 5. Phase-space plots: **(a)** unperturbed plot and **(b)** perturbed plot for $A = 0.2$, $D = 0.005$, $J = 12$, $S = 0.5$, $\epsilon = 0.5$, $x = 0.0381591$, $p_x = -0.0120476$.

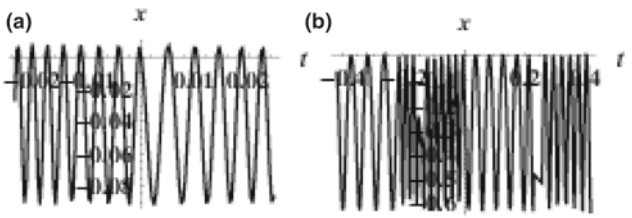

Figure 6. Trajectory plots: **(a)** unperturbed plot and **(b)** perturbed plot for $A = 0.2$, $D = 0.005$, $J = 12$, $S = 0.5$, $\epsilon = 0.5$, $x = 0.0381591$, $p_x = -0.0120476$.

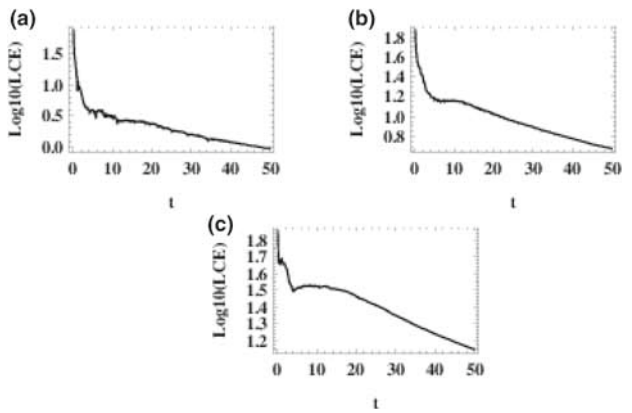

Figure 7. Lyapunov curves in terms of displacement perturbation for $A = 0.2$, $D = 0.005$, $J = 12$, $S = 0.5$, $\epsilon = 0.5$ at **(a)** 10^{-12}, **(b)** 10^{-13} and **(c)** 10^{-14}.

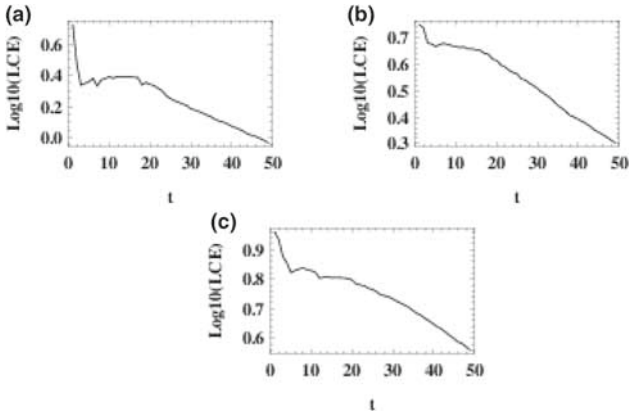

Figure 8. Lyapunov curves in terms of momentum perturbation for $A = 0.2$, $D = 0.005$, $J = 12$, $S = 0.5$, $\epsilon = 0.5$ at **(a)** 10^{-12}, **(b)** 10^{-13} and **(c)** 10^{-14}.

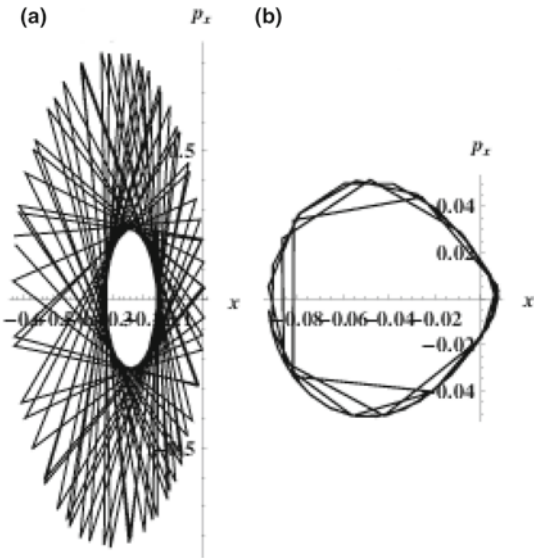

Figure 9. Phase-space plots: **(a)** unperturbed plot **(b)** perturbed plot for $A = 0.2$, $D = 0.007$, $J = 12$, $S = 0.5$, $\epsilon = 0.5$, $x = 0.0381591$, $p_x = -0.0120476$.

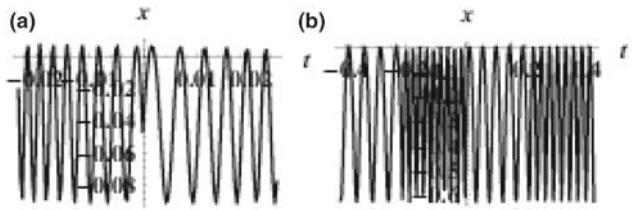

Figure 10. Trajectory plots: **(a)** unperturbed plot and **(b)** perturbed plot for $A = 0.2$, $D = 0.007$, $J = 12$, $S = 0.5$, $\epsilon = 0.5$, $x = 0.0381591$, $p_x = -0.0120476$.

Case (ii) $D = 0.007$: The unperturbed curve when $D = 0.007$ has overlapped spikes, moving in a periodic motion. Increasing the D–M interaction energy makes the spikes separable and the star-like gesture disappears. The perturbed plot (figure 9b) indicates more expansion of oscillations from the cross well pattern. On analysing

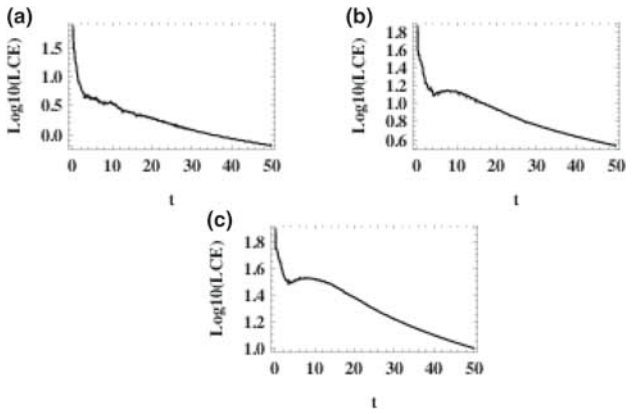

Figure 11. Lyapunov curves in terms of displacement perturbation for $A = 0.2$, $D = 0.007$, $J = 12$, $S = 0.5$, $\epsilon = 0.5$ at **(a)** 10^{-12}, **(b)** 10^{-13} and **(c)** 10^{-14}.

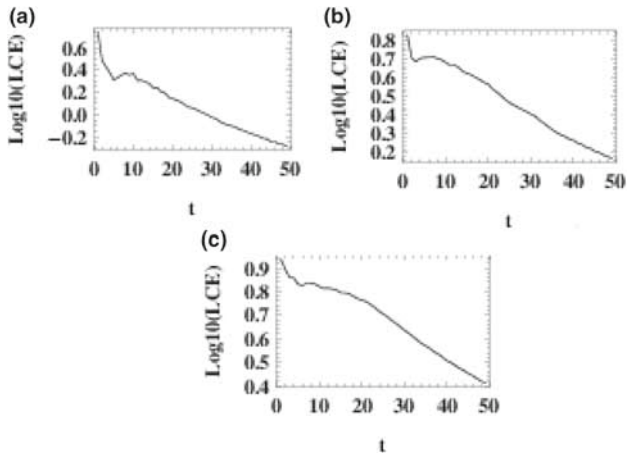

Figure 12. Lyapunov curves in terms of momentum perturbation for $A = 0.2$, $D = 0.007$, $J = 12$, $S = 0.5$, $\epsilon = 0.5$ at **(a)** 10^{-12}, **(b)** 10^{-13} and **(c)** 10^{-14}.

the trajectories given in figure 10, the unperturbed time series plot shows periodic behaviour with non-sticky trajectories. Figure 10b depicts the perturbed curve which loses its minor nonlinearity factor that appears at the centre of the axis due to perturbation. Here the trajectories were sticky with decayed amplitude which oscillate periodically, resulting in a linear harmonic oscillator.

Figures 11 and 12 depict the Lyapunov spectra for $D = 0.007$. By varying the perturbation values from 10^{-12}, 10^{-13} and 10^{-14}, the plots are constructed. From the Lyapunov plots, it is found that as the size of perturbation increases, the Lyapunov exponent increases simultaneously. They are positive. It confirms the presence of chaos in the ferromagnetic system with the combined action of the dipole–dipole and D–M interactions.

3. Model Hamiltonian for ferromagnetic spin chain with quadrupole–quadrupole and D–M interactions

By incorporating the quadrupole–quadrupole interaction in the FM system, we write the Hamiltonian in the following form:

$$H = -\sum_i [\tilde{J}(\vec{S}_i \cdot \vec{S}_{i+1}) + \tilde{J}'(\vec{S}_i \cdot \vec{S}_{i+1})^2 + \tilde{D}\vec{Z} \cdot (\vec{S}_i \times \vec{S}_{i+1}) - \tilde{A}(S_i^z)^2 - \tilde{A}'(S_i^z)^4]. \quad (11)$$

In eq. (11), A' is the higher-order uniaxial anisotropic energy, its easy axis of magnetisation is chosen along the z-direction and J' is the biquadratic isotropic exchange interaction [33]. For further calculations, we rewrite the above equation in dimensionless form as follows:

$$\begin{aligned} H = -\sum_i \Bigg[& \frac{J}{2S^2}\left(\hat{S}_i^+ \hat{S}_{i+1}^- + \hat{S}_i^- \hat{S}_{i+1}^+ + 2\hat{S}_i^z \hat{S}_{i+1}^z\right) \\ & + \frac{J'}{4S^4}\left(\hat{S}_i^+ \hat{S}_{i+1}^- \hat{S}_i^+ \hat{S}_{i+1}^- + \hat{S}_i^+ \hat{S}_{i+1}^- \hat{S}_i^- \hat{S}_{i+1}^+ \right. \\ & + \hat{S}_i^- \hat{S}_{i+1}^+ \hat{S}_i^+ \hat{S}_{i+1}^- + \hat{S}_i^- \hat{S}_{i+1}^+ \hat{S}_i^- \hat{S}_{i+1}^+ \\ & + 4\hat{S}_i^+ \hat{S}_{i+1}^- \hat{S}_i^z \hat{S}_{i+1}^z + 4\hat{S}_i^- \hat{S}_{i+1}^+ \hat{S}_i^z \hat{S}_{i+1}^z \\ & \left. + 4\hat{S}_i^z \hat{S}_{i+1}^z \hat{S}_i^z \hat{S}_{i+1}^z\right) + \frac{D}{2iS^2}\left(-\hat{S}_i^+ \hat{S}_{i+1}^- + \hat{S}_i^- \hat{S}_{i+1}^+\right) \\ & - \frac{A}{S^2}\left(\hat{S}_i^z\right)^2 - \frac{A'}{S^4}\left(\hat{S}_i^z\right)^4 \Bigg]. \end{aligned} \quad (12)$$

3.1 *Semiclassical approach*

Following the same procedure as in §2.1 we bosonise eq. (12) using eq. (3), which gives

$$\begin{aligned} H = \Bigg[& A + A' - J - J' \\ & - \frac{1}{S}\left(2Aa_n a_n^\dagger - Ja_n a_n^\dagger - 2J'a_n a_n^\dagger \right. \\ & \left. - Ja_{n+1}\, a_{n+1}^\dagger - 2J'a_{n+1}a_{n+1}^\dagger\right) \\ & + \frac{1}{S^2}\left(Aa_n^2 a_n^{\dagger 2} - J'a_n^2\, a_n^{\dagger 2} - Ja_n a_{n+1} a_n^\dagger a_{n+1}^\dagger \right. \\ & \left. + 4J'a_n a_{n+1} a_n^\dagger a_{n+1}^\dagger - J'a_{n+1}^2\, a_{n+1}^{\dagger 2}\right) \\ & - \frac{1}{S^3}\left(2J'a_n^2\, a_{n+1}\, a_n^{\dagger 2} a_{n+1}^\dagger + 2J'a_n a_{n+1}^2 a_n^\dagger a_{n+1}^{\dagger 2}\right) \\ & - \frac{1}{S^4}J'a_n^2\, a_{n+1}^2\, a_n^{\dagger 2}\, a_{n+1}^{\dagger 2} - \epsilon^2\Big[iDa_{n+1}a_i^\dagger \\ & - Ja_{n+1}a_n^\dagger - 2J'a_{n+1}a_n^\dagger - iDa_n a_{n+1}^\dagger \end{aligned}$$

$$
\begin{aligned}
&- J a_n a_{n+1}^{\dagger} - 2J' a_n a_{n+1}^{\dagger} \\
&+ \frac{1}{S}\Big(2J' a_n a_{n+1}\, a_n^{\dagger 2} + 2J' a_n^2 a_n^{\dagger} a_{n+1}^{\dagger} \\
&+ 2J' a_{n+1}^2\, a_n^{\dagger}\, a_{n+1}^{\dagger} + 2J' a_n a_{n+1} a_{n+1}^{\dagger 2}\Big) \\
&- \frac{1}{S^2}\Big(2J' a_n a_{n+1}^2 a_n^{\dagger 2}\, a_{n+1}^{\dagger} \\
&+ 2J' a_n^2 a_{n+1} a_n^{\dagger} a_{n+1}^{\dagger 2}\Big)\Big]\epsilon^4\Big[\frac{1}{4}\Big(-iD a_n a_{n+1} a_n^{\dagger 2} \\
&+ J a_n a_{n+1} a_n^{\dagger 2} + iD a_n^2 a_n^{\dagger} a_{n+1}^{\dagger} + J a_n^2 a_n^{\dagger} a_{n+1}^{\dagger} \\
&- iD a_{n+1}^2 a_n^{\dagger} a_{n+1}^{\dagger} + J a_{n+1}^2 a_n^{\dagger} a_{n+1}^{\dagger} \\
&+ iD a_n a_{n+1} a_{n+1}^{\dagger 2} + J a_n a_{n+1} a_{n+1}^{\dagger 2}\Big) \\
&+ \frac{1}{2}\Big(J' a_n a_{n+1} a_n^{\dagger 2} + J' a_n^2 a_n^{\dagger} a_{n+1}^{\dagger} + J' a_{n+1}^2 a_n^{\dagger} a_{n+1}^{\dagger} \\
&+ J' a_n a_{n+1} a_{n+1}^{\dagger 2}\Big) - J' a_{n+1}^2 a_n^{\dagger 2} \\
&- 2J' a_n a_{n+1} a_n^{\dagger} a_{n+1}^{\dagger} - J' a_n^2 a_{n+1}^{\dagger 2} \\
&+ \frac{1}{S}\Big(-\frac{1}{2} J' a_n^2 a_{n+1} a_n^{\dagger 3} - \frac{1}{2} J' a_n^3\, a_n^{\dagger 2} a_{n+1}^{\dagger} \\
&- J' a_n a_{n+1}^2 a_n^{\dagger 2} a_{n+1}^{\dagger} - J' a_n^2 a_{n+1} a_n^{\dagger} a_{n+1}^{\dagger 2} \\
&- \frac{1}{2} J' a_{n+1}^3\, a_n^{\dagger} a_{n+1}^{\dagger 2} - J' a_n a_{n+1}^2 a_{n+1}^{\dagger 3}\Big) \\
&+ \frac{1}{2S^2}\Big(J' a_n^2 a_{n+1}^2 a_n^{\dagger 3}\, a_{n+1}^{\dagger} + J' a_n^3\, a_{n+1} a_n^{\dagger 2}\, a_{n+1}^{\dagger 2} \\
&+ J' a_n a_{n+1}^3 a_n^{\dagger 2}\, a_{n+1}^{\dagger 2} + J' a_n^2 a_{n+1}^2 a_n^{\dagger} a_{n+1}^{\dagger 3}\Big)\Big] \\
&- \frac{1}{S} 4\, a_n a_n^{\dagger} A' + \frac{1}{S^2} 6\, a_n^2 a_n^{\dagger 2} A' \\
&- \frac{1}{S^3}\, 4\, a_n^3\, a_n^{\dagger 3} A' + \frac{1}{S^4} a_n^4\, a_n^{\dagger 4} J'\Big]. \qquad (13)
\end{aligned}
$$

For the chaotic dynamical study, the first quantised form of eq. (13) is calculated by using eq. (5). It is presented as

$$
\begin{aligned}
H = {} & A + A' - J - J' + \frac{1}{S} E_1 \\
& + \frac{1}{S^2} E_2 + \frac{1}{S^3} E_3 + \frac{1}{S^4} E_4 \\
& + \epsilon^2\Big[F_1 + \frac{1}{S} F_2 + \frac{1}{S^2} F_3\Big] \\
& + \epsilon^4\Big[G_1 + \frac{1}{S} G_2 + \frac{1}{S^2} G_3\Big], \qquad (14)
\end{aligned}
$$

Table 4. Fixed points.

S. No.	x	p_x
(i)	−0.911615	0.00000115
(ii)	−0.252003	0.000000529
(iii)	−0.250168	−0.375017

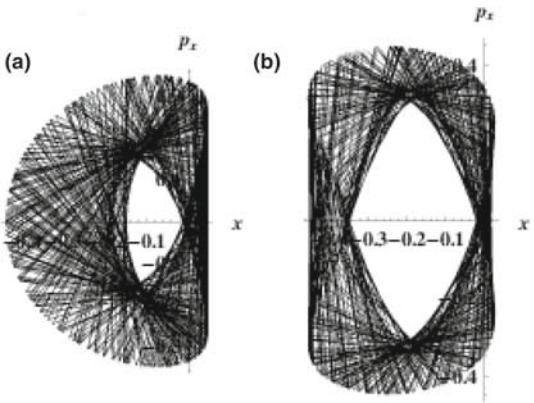

Figure 13. Phase-space plots: **(a)** unperturbed plot and **(b)** perturbed plot for $A = 0.2$, $A' = 2.05$, $D = 0.001$, $J = 12$, $J' = 6$, $S = 0.5$, $\epsilon = 0.5$, $x = -0.911615$, $p_x = 0.00000115$.

where the values of E_1, E_2, E_3, E_4, F_1, F_2, F_3, G_1, G_2 and G_3 are given in Appendix A.

3.2 *Hamilton's equations of motion*

The equations of motion for the quadrupole–quadrupole-type interaction are formulated using eqs (7) and (8). They are given in Appendix B.

3.3 *Phase plots and irregular trajectories*

From the derived Hamilton's equations of motion, fixed points are calculated and are tabulated in table 4. For the perturbation analysis, we chose $x = -0.911615$, $p_x = 0.00000115$. The phase-space portraits obtained are displayed in figures 13 and 14. In the original system, the unperturbed plot obtained is a rosette-shaped orbit with a curled corner facing backwards. It approaches the negative scale. The orbit has an infinite number of periodic waves with a small elongated space inside. But with added perturbation, the short pyriform-shaped plot in the system with dipole–dipole interaction energy turns into a cylindrical-shaped orbit due to the effect of quadrupole–quadrupole interaction energy. It has curled corners at both the ends.

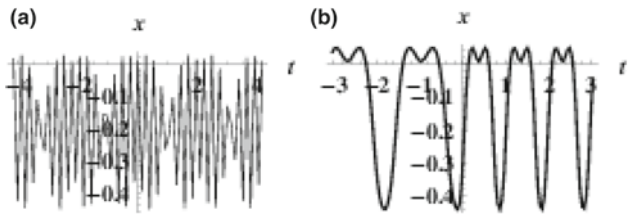

Figure 14. Trajectory plots: **(a)** unperturbed plot and **(b)** perturbed plot for $A = 0.2$, $A' = 2.05$, $D = 0.001$, $J = 12$, $J' = 6$, $S = 0.5$, $\epsilon = 0.5$, $x = -0.911615$, $p_x = 0.00000115$.

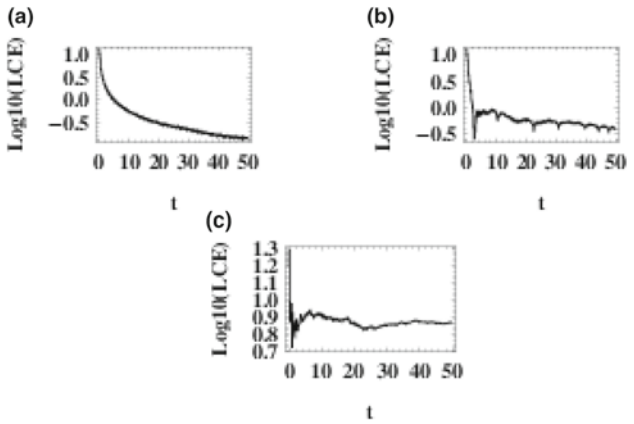

Figure 15. Lyapunov curves in terms of displacement perturbation for $A = 0.2$, $A' = 2.05$, $D = 0.001$, $J = 12$, $J' = 6$, $S = 0.5, \epsilon = 0.5$ at **(a)** 10^{-10}, **(b)** 10^{-12} and **(c)** 10^{-14}.

The time series evolution plot is shown in figure 14. When there is no perturbation, the trajectory is visualised as a quasiperiodic attractor. In figure 14b we notice a modulation in the frequency of oscillation. Furthermore, amplitudes of both the top and bottom layers of oscillations are in good agreement with definite accuracy. It behaves as a harmonic oscillator.

3.3.1 *Lyapunov stability analysis.* Similarly, as in the system with bilinear and D–M interactions, the system with biquadratic and D–M interactions is further tested for stability.

Case (i) *Displacement perturbation*: Figure 15 represents the LCE curves for the impact of the quadrupole–quadrupole-type interaction. In this work, while perturbing the displacement, the system becomes stable and the chaotic behaviour is lost due to the addition of D–M interaction along with quadrupole–quadrupole interaction. Table 5 gives MLE values for different displacement perturbations.

Case (ii) *Momentum perturbation*: The logarithmic plot of the Lyapunov exponent for momentum perturbation

Table 5. MLE for different displacement perturbation.

S. No.	Size of perturbation	MLE
(a)	10^{-10}	−0.4
(b)	10^{-12}	−0.5
(c)	10^{-14}	0.7

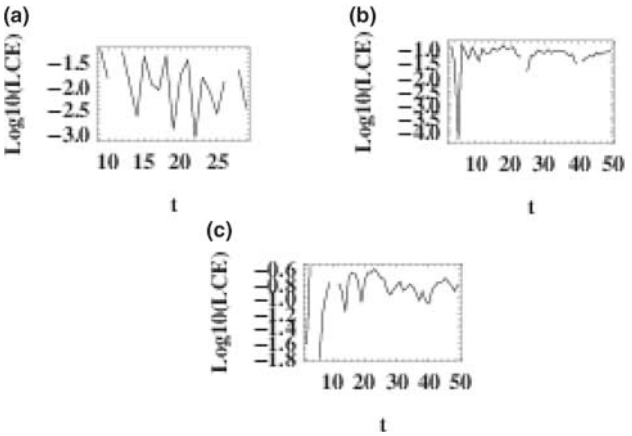

Figure 16. Lyapunov curves in terms of momentum perturbation for $A = 0.2$, $A' = 2.05$, $D = 0.001$, $J' = 6$, $J = 12$, $S = 0.5, \epsilon = 0.5$ at **(a)** 10^{-10}, **(b)** 10^{-11} and **(c)** 10^{-12}.

Table 6. MLE for different momentum perturbation.

S. No.	Size of perturbation	MLE
(a)	10^{-10}	−3.0
(b)	10^{-11}	−4.0
(c)	10^{-12}	−1.8

is displayed in figure 16. It is noticed that when momentum is perturbed, the system is more stable and all the calculated MLE values become negative. The chaotic behaviour is not observed in this system. The MLE values for different sizes of momentum perturbation are tabulated in table 6.

3.4 *Influence of the D–M interaction with the quadrupole–quadrupole-type interaction*

In this study D takes the values 0.005 and 0.007.

Case (i) $D = 0.005$: Figures 17a and 17b are the phase-space plots for the given system. It is observed that when the system is unperturbed, the rosette-shaped orbit displays patches at certain regions. The effect of interaction energy also makes the curled corners to move more towards the positive scale. When a small

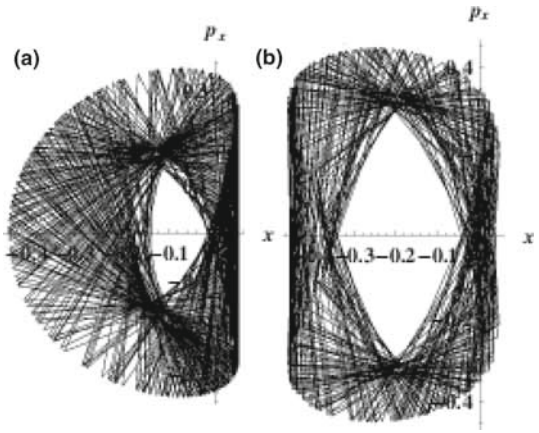

Figure 17. Phase-space plots: **(a)** unperturbed plot and **(b)** perturbed plot for $A = 0.2$, $A' = 2.05$, $D = 0.005$, $J = 12$, $J' = 6$, $S = 0.5$, $\epsilon = 0.5$, $x = -0.911615$, $p_x = 0.00000115$.

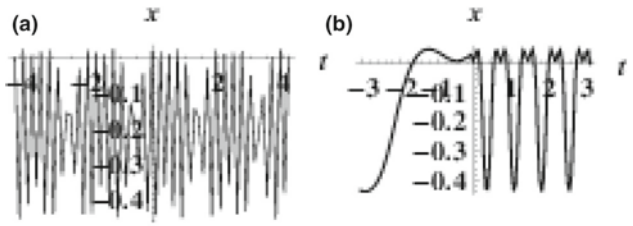

Figure 18. Trajectory plots: **(a)** unperturbed plot and **(b)** perturbed plot for $A = 0.2$, $A' = 2.05$, $D = 0.005$, $J = 12$, $J' = 6$, $S = 0.5$, $\epsilon = 0.5$, $x = -0.911615$, $p_x = 0.00000115$.

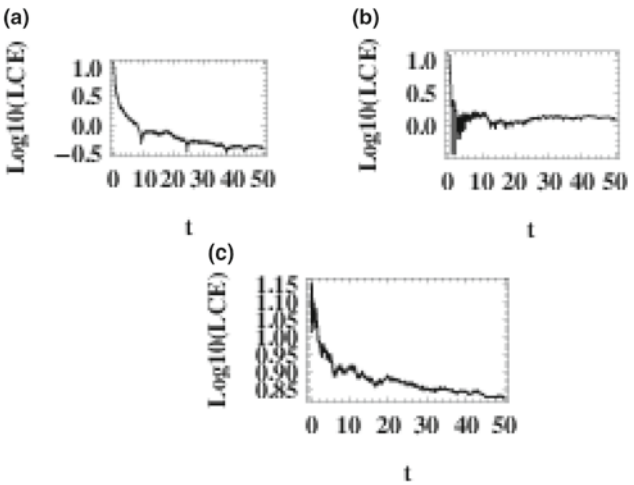

Figure 19. Lyapunov curves in terms of displacement perturbation for $A = 0.2$, $A' = 2.05$, $D = 0.005$, $J = 12$, $J' = 6$, $S = 0.5, \epsilon = 0.5$ at **(a)** 10^{-12}, **(b)** 10^{-13} and **(c)** 10^{-14}.

perturbation $x = -0.911615$ and $p_x = 0.00000115$ are added, the phase-space plot obtained is a cylindrical-shaped orbit. To ensure accuracy, we examine the

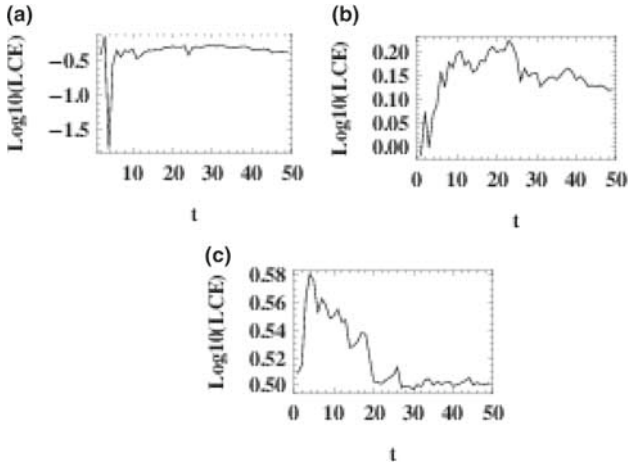

Figure 20. Lyapunov curves in terms of momentum perturbation for $A = 0.2$, $A' = 2.05$, $D = 0.005$, $J = 12$, $J' = 6$, $S = 0.5$, $\epsilon = 0.5$ at **(a)** 10^{-12}, **(b)** 10^{-13} and **(c)** 10^{-14}.

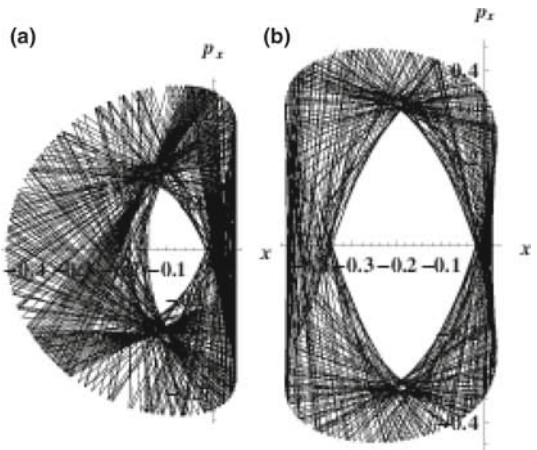

Figure 21. Phase-space plots: **(a)** unperturbed plot and **(b)** perturbed plot for $A = 0.2$, $A' = 2.05$, $D = 0.007$, $J = 12$, $J' = 6$, $S = 0.5$, $\epsilon = 0.5$, $x = -0.911615$, $p_x = 0.00000115$.

time series evolution plots. The unperturbed trajectory (figure 18a) is observed as a quasiperiodic attractor. However, the perturbed plot shown in figure 18b has more variation in frequency followed by a complexity of oscillation that bounces over the negative scale behaving anharmonically.

The Lyapunov spectrum of the system for $D = 0.005$ in terms of perturbation in displacement and momentum is studied to find out the stability. The effect of perturbation at 10^{-12}, 10^{-13} and 10^{-14} is displayed in figures 19 and 20. They portray the nature of hyperchaos.

Case (ii) $D = 0.007$: The phase-space portraits for this system with $D = 0.007$ are presented in figures 21 and 22. The patches formed in figure 17a tend to disappear

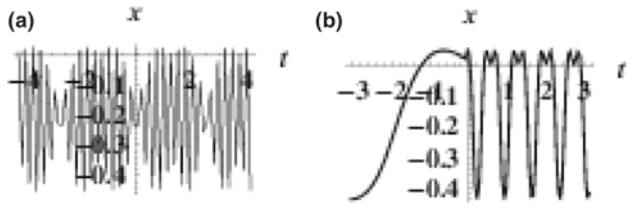

Figure 22. Trajectory plots: **(a)** unperturbed plot and **(b)** perturbed plot for $A = 0.2$, $A' = 2.05$, $D = 0.007$, $J = 12$, $J' = 6$, $S = 0.5$, $\epsilon = 0.5$, $x = -0.911615$, $p_x = 0.00000115$.

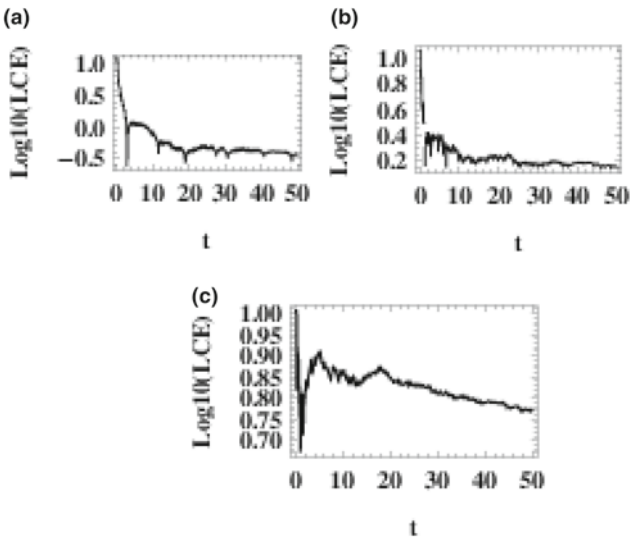

Figure 23. Lyapunov curves in terms of displacement perturbation for $A = 0.2$, $A' = 2.05$, $D = 0.007$, $J = 12$, $J' = 6$, $S = 0.5, \epsilon = 0.5$ at **(a)** 10^{-12}, **(b)** 10^{-13} and **(c)** 10^{-14}.

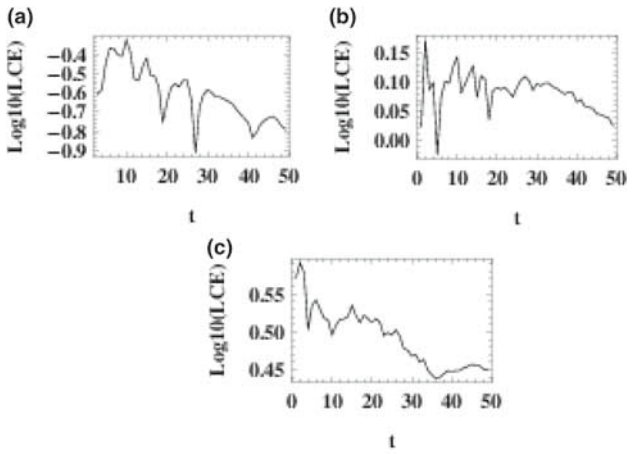

Figure 24. Lyapunov curves in terms of momentum perturbation for $A = 0.2$, $A' = 2.05$, $D = 0.007$, $J = 12$, $J' = 6$, $S = 0.5, \epsilon = 0.5$ at **(a)** 10^{-12}, **(b)** 10^{-13} and **(c)** 10^{-14}.

due to the D–M interaction which is shown in figure 21a. In the perturbed plot, only the flipped ends shift towards the positive end. Figure 22a is evidently quasiperiodic and the perturbed trajectory in figure 22b shows anharmonic behaviour.

The Lyapunov characteristic exponent described in figures 23 and 24 shows that the system with quadrupole–quadrupole-type interaction combining very low D–M interaction energy will be in a stable state and so the chaotic nature is absent. As the D–M interaction energy increases, the system becomes unstable leading to hyperchaos.

4. Conclusion

This paper deals with the chaotic dynamics of a one-dimensional Heisenberg ferromagnetic spin chain comprising dipole–dipole, quadrupole–quadrupole and D–M interactions. In this study, we write a model Hamiltonian in the sequential quantised form which is then remodelled into the first quantised form to analyse its chaotic behaviour. Phase-space portraits are drawn and a comparative study using the effect of D–M interaction is demonstrated. Moreover, the Lyapunov stability analysis is carried out and the plots are illustrated graphically. Finally, we found that the system with dipole–dipole interaction energy symbolises the phase-space plots with chaotic patterns and the trajectories to progress periodically. The influence of quadrupole–quadrupole interaction energy and D emphasises trajectories as quasiperiodic. The Lyapunov curves exhibit hyperchaotic nature under specific conditions.

Acknowledgements

This work forms part of a major research project sponsored by the Science and Engineering Research Board, Department of Science and Technology, Government of India (No. EMR/2015/001884).

Appendix A

The coefficients of eq. (14) are

$$E_1 = h^2Ja^2 + 2hJxa^2 - 2Ax^2a^2 + 2Jx^2a^2 + 2Ap_xb^2 - 2Jp_x^2b^2 + 2h^2a^2J' + 4hxa^2J' + 4x^2a^2J' - 4p_x^2b^2J' - 4x^2a^2A' + 4p_x^2b^2A',$$

$$E_2 = -h^2Jx^2a^4 - 2hJx^3a^4 + Ax^4a^4 - Jx^4a^4 + h^2Jp_x^2a^2b^2 + 2hJp_x^2xa^2b^2 - 2Ap_x^2a^2b^2$$

$$
\begin{aligned}
&+2Jp_x^2x^2a^2b^2 + Ap_x^4b^4 - Jp_x^4b^4 - h^4a^4J' \\
&-4h^3xa^4J' - 10h^2x^2a^4J' - 12hx^3a^4J' \\
&-6x^4a^4J' - 6h^2p_x^2a^2b^2J' + 12hp_x^2xa^2b^2J' \\
&+12p_x^2x^2a^2b^2J' - 6p_x^4b^4J' + 6x^4a^4A' \\
&+12p_x^2x^2a^2b^2A' + 6p_x^4b^4J', \\
E_3 = {}& 2h^4x^2a^6J' + 8h^3x^3a^6J' + 14h^2x^4a^6J' \\
&+12hx^5a^6J' + 4x^6a^6J' + 2h^4p_x^2a^4b^2J' \\
&+8h^3p_x^2xa^4b^2J' + 20h^2p_x^2x^2a^4b^2J' \\
&+24hp_x^2x^3a^4b^2J' + 12p_x^2x^4a^4b^2J' \\
&+6h^2p_x^4b^4J' + 12hp_x^4xa^2b^4J' \\
&+12p_x^4x^2a^2b^4J' - 4p_x^6b^6J' - 4x^6a^6A' \\
&-12p_x^2x^4a^4b^2A' - 12p_x^4x^2b^4A' \\
&-4p_x^6b^6A', \\
E_4 = {}& -h^4x^4a^8J' - 4h^3x^5a^8J' - 6h^2x^6a^8J' \\
&-4hx^7a^8J' - x^8a^8J' - 2h^4p_x^2x^2a^6b^2J' \\
&-8h^3p_x^2x^3a^6b^2J' - 14h^2p_x^2x^4a^6b^2J' \\
&-12hp_x^2x^5a^6b^2J' - 4p_x^2x^6a^6b^2J' \\
&-h^4p_x^4a^4b^4J' - 4h^3p_x^4xa^4b^4J' \\
&-10h^2p_x^4x^2a^4b^4J' - 12hp_x^4x^3a^4b^4J' \\
&-6p_x^4x^4a^4b^4J' - 2h^2p_x^6a^2b^6J' \\
&-4hp_x^6xa^2b^6J' - 4p_x^6x^2a^2b^6J' - p_x^8b^8J' \\
&+x^8a^8A' + 4p_x^3x^6a^6b^2A' + 6p_x^4x^4a^4b^4A' \\
&+4p_x^6x^2a^2b^6A' + p_x^8b^8A', \\
F_1 = {}& -2hJxa^2 - 2Jx^2a^2 + 2Dhp_xab - 2Jp_x^2b^2 \\
&-4hxa^2f_i'J' - 4x^2a^2J' + 4p_x^2b^2J', \\
F_2 = {}& 4h^3xa^4J' + 12h^2x^2a^4J' + 16hx^3a^4J' \\
&+8x^4a^4J' - 4h^2p_x^2a^2b^2J' - 16hp_x^2xa^2b^2J' \\
&-16p_x^2x^2a^2b^2J' + 8p_x^4b^4J', \\
F_3 = {}& -4h^3x^3a^6J' - 12h^2x^4a^6J' - 12hx^5a^6J' \\
&-4x^6a^6J' + 4h^3p_x^2xa^4b^2J' \\
&+16h^2i^2p_x^2x^2a^4b^2J' + 24hp_x^2x^3a^4b^2J' \\
&+12p_x^2x^3a^4b^2J' - 4h^2p_x^4a^2b^4J' \\
&-12hp_x^4xa^2b^4J' - 12p_x^4x^2a^2b^4J' \\
&+4p_x^6b^6J', \\
G_1 = {}& 2hJx^3a^4 + Jx^4a^4 - Dh^2p_xxa^3b \\
&-Dhp_xx^2a^3b + 2hi^2Jp_x^2xa^2b^2 \\
&+2Jp_x^2x^2a^2b^2 - Dhp_x^3ab^3 + Jp_x^4b^4 \\
&+h^3xa^4J' - h^2x^2a^4J' - 4hx^3a^4J' \\
&-2x^4a^4J' + h^2p_x^2a^2b^2J' - 4hp_x^2xa^2b^2J' \\
&-4p_x^2x^2a^2b^2J' - 2p_x^4b^4J' \\
&+\frac{1}{2}\Big(h^3Ja^4x + 3h^2Jx^2a^4 \\
&-Dh^3p_xa^3b + h^2i^2Jp_x^2a^2b^2\Big), \\
G_2 = {}& -h^5xa^6J' - 5h^4x^2a^6J' \\
&-12h^3x^3a^6J' - 16h^2x^4a^6J' \\
&-12hx^6a^6J' - 4x^6a^6J' - h^4p_x^2a^4b^2J' \\
&-8h^3p_x^2xa^4b^2J' - 20h^2p_x^2x^2a^4b^2J' \\
&-24hp_x^2x^3a^4b^2J' - 12p_x^2x^4a^4b^2J' \\
&-4h^2p_x^4a^2b^4J' - 12hp_x^4xa^2b^4J' \\
&-12p_x^4x^2a^2b^4J' - 4p_x^6b^6J', \\
G_3 = {}& h^5x^3a^8J' + 5h^4x^4a^8J' + 11h^3x^5a^8J' \\
&+13h^2x^6a^8J' + 8hx^7a^8J' + 2x^8a^8J' \\
&-h^5p_x^2xa^6b^2J' + 6h^4p_x^2x^2a^6b^2J' \\
&+18h^3p_x^2x^3a^6b^2J' + 29h^2p_x^2x^4a^6b^2J' \\
&+24hp_x^2x^5a^5b^2J' + 8p_x^2x^6a^6b^2J' \\
&+h^4p_x^4a^4b^4J' + 7h^3p_x^4xa^4b^4J' \\
&+19h^2p_x^4x^2a^4b^4J' + 24hp_x^4x^3a^4b^4J' \\
&+12p_x^4x^4a^4b^4J' + 3h^2p_x^6a^2b^6J' \\
&+8hp_x^6xa^2b^6J' + 8p_x^6x^2a^2b^6J' \\
&+2p_x^8b^8J'.
\end{aligned}
$$

Appendix B

$$
\begin{aligned}
\frac{\mathrm{d}x}{\mathrm{d}t} = {}& \frac{1}{S}\Big(-4Ap_xb^2 + 4Jp_xb^2 + 8p_xb^2J' \\
&-8p_xb^2A'\Big) - \frac{1}{S^2}\Big(2h^2Jp_xa^2b^2
\end{aligned}
$$

$$
\begin{aligned}
&-4hJp_x x a^2 b^2 + 4Ap_x x^2 a^2 b^2 \\
&-4Jp_x x^2 a^2 b^2 + 4Ap_x^3 b^4 \\
&-4Jp_x^3 b^4 - 12h^2 p_x a^2 b^2 J' \\
&-24hp_x x a^2 b^2 J' - 24p_x x^2 a^2 b^2 J' \\
&-24p_x^3 b^4 J' + 24p_x x^2 a^2 b^2 A' + 24p_x^3 b^4 A'\Big) \\
&+\frac{1}{S^3}\Big(4h^4 p_x a^4 b^2 J' + 16h^3 p_x x a^4 b^2 J' \\
&+40h^2 p_x x^2 a^4 b^2 J' + 48hp_x x^3 a^4 b^2 J' \\
&+24p_x x^4 a^4 b^2 J' + 24h^2 p_x^3 a^2 b^4 J' \\
&+48hp_x^3 x a^2 b^4 J' + 48p_x^3 x^2 a^2 b^4 J' \\
&+24p_x^5 b^6 J' - 24p_x x^4 a^4 b^2 A' \\
&-48p_x^3 x^2 a^2 b^4 A' - 24p_x^5 b^6 A'\Big) \\
&+\frac{1}{S^4}\Big(-4h^4 p_x x^2 a^6 b^2 J' - 16h^3 p_x x^3 a^6 b^2 J' \\
&-28h^2 p_x x^4 a^6 b^2 J' - 24hp_x x^5 a^6 b^2 J' \\
&-8p_x x^6 a^6 b^2 J' - 4h^4 p_x^3 a^4 b^4 J' \\
&-16h^3 p_x^3 x a^4 b^4 J' - 40h^2 p_x^3 x^2 a^4 b^4 J' \\
&-48hp_x^3 x^3 a^4 b^4 J' - 24p_x^3 x^4 a^4 b^4 J' \\
&-12h^2 p_x^5 a^2 b^6 J' - 24hp_x^5 x a^2 b^6 J' \\
&-24p_x^5 x^2 a^2 b^6 J' - 8p_x^7 b^8 J' \\
&+8p_x x^6 a^6 b^2 A' + 24p_x^3 x^4 a^4 b^4 A' \\
&+24p_x^5 x^2 a^2 b^6 A' + 8p_x^7 b^8 A'\Big) \\
&+\epsilon^2\Big(2Dhab - 4Jp_x b^2 - 8p_x b^2 J' \\
&+\frac{1}{S}\Big(8h^2 p_x a^2 b^2 J' + 32hp_x x a^2 b^2 J' \\
&+32p_x x^2 a^2 b^2 J' + 32p_x^3 b^4 J'\Big) \\
&+\frac{1}{S^2}\Big(-8h^3 p_x x a^4 b^2 J' - 32h^2 p_x x^2 a^4 b^2 J' \\
&-48hp_x x^3 a^4 b^2 J' - 24p_x x^4 a^4 b^2 J' \\
&-16h^2 p_x^3 a^2 b^4 J' - 48hp_x^3 x a^2 b^4 J' \\
&-48p_x^3 x^2 a^2 b^4 J' - 24p_x^5 b^6 J'\Big)\Big) \\
&+\epsilon^4\Big(-\frac{1}{2}Dh^3 a^3 b - Dh^2 x a^3 b - Dhx^2 a^3 b \\
&+h^2 Jp_x a^2 b^2 + 4hJp_x x a^2 b^2 + 4Jp_x x^2 a^2 b^2 \\
&-3Dhp_x^2 a b^3 + 4Jp_x^3 b^4 + 2h^2 p_x a^2 b^2 J' \\
&-8hp_x x a^2 b^2 J' - 8p_x x^2 a^2 b^2 J' - 8p_x^3 b^4 J' \\
&+\frac{1}{S}\Big(-2h^4 p_x a^4 b^2 J' - 16h^3 p_x x a^4 b^2 J' \\
&-40h^2 p_x x^2 a^4 b^2 J' - 48hp_x x^3 a^4 b^2 J' \\
&-24p_x x^4 a^4 b^2 J' - 16h^2 p_x^3 a^2 b^4 J' \\
&-48h p_x^3 x a^2 b^4 J' - 48p_x^3 x^2 a^2 b^4 J' \\
&-24p_x^5 b^6 J'\Big) \\
&+\frac{1}{S^2}\Big(2h^5 p_x x a^6 b^2 J' + 12h^4 p_x x^2 a^6 b^2 J' \\
&+36h^3 p_x x^3 a^6 b^2 J' + 58h^2 p_x x^4 a^6 b^2 J' \\
&+48hp_x x^5 a^6 b^2 J' + 16p_x x^6 a^6 b^2 J' \\
&+4h^4 p_x^3 a^4 b^4 J' + 28h^3 p_x^3 x a^4 b^4 J' \\
&+76h^2 p_x^3 x^2 a^4 b^4 J' + 96hp_x^3 x^3 a^4 b^4 J' \\
&+48p_x^3 x^4 a^4 b^4 J' + 18h^2 p_x^5 a^2 b^6 J' \\
&+48hp_x^5 x a^2 b^6 J' + 48p_x^5 x^2 a^2 b^6 J' \\
&+16p_x^7 b^8 J'\Big)\Big), \qquad (15)
\end{aligned}
$$

$$
\begin{aligned}
\frac{\mathrm{d}p_x}{\mathrm{d}t} = &\frac{1}{S}\Big(2hJa^2 - 4Axa^2 + 4Jxa^2 + 4ha^2 J' \\
&+8xa^2 J' + 8xa^2 A'\Big) \\
&+\frac{1}{S^2}\Big(-2h^2 Jxa^4 - 6hJx^2 a^4 + 4Ax^3 a^4 \\
&-4Jx^3 a^4 - 2hJp_x^2 a^2 b^2 + 4Ap_x^2 x a^2 b^2 \\
&-4Jp_x^2 x a^2 b^2 - 4h^3 a^4 J' - 20h^2 x a^4 J' \\
&-36hx^2 a^4 J' - 24x^3 a^4 J' - 12hp_x^2 a^2 b^2 J' \\
&-24p_x^2 x a^2 b^2 J' - 24x^3 a^4 A' \\
&+24p_x^2 x a^2 b^2 A'\Big) \\
&+\frac{1}{S^3}\Big(4h^4 x a^6 J' + 24h^3 x^3 a^6 J' + 56h^2 x^3 a^6 J' \\
&+60hx^4 a^6 J' + 24x^5 a^6 J' + 8h^3 p_x^2 a^4 b^2 J' \\
&+40h^2 p_x^2 x a^4 b^2 J' + 72hp_x^2 x^2 a^4 b^2 J' \\
&+48p_x^2 x^3 a^4 b^2 J' + 12hp_x^4 a^2 b^4 J' \\
&+24p_x^4 x a^2 b^4 J' 24x^5 a^6 A' - 48p_x^2 x^3 a^4 b^2 A' \\
&+24p_x^4 x a^2 b^4 A'\Big) + \frac{1}{S^4}\Big(-4h^4 x^3 a^8 J' \\
&-20h^3 x^4 a^8 J' - 36h^2 x^5 a^8 J' - 28hx^6 a^8 J'
\end{aligned}
$$

$$
\begin{aligned}
&-8x^7a^8J'-4h^4p_x^2xa^6b^2J'\\
&-24h^3p_x^2x^2a^6b^2J'\\
&-56h^2p_x^2x^3a^6b^2J'-60hp_x^2x^4a^6b^2J'\\
&-24p_x^2x^5a^6b^2J'-4h^3p_x^4a^4b^4J'\\
&-20h^2p_x^4xa^4b^4J'-36hp_x^4x^2a^4b^4J'\\
&-24p_x^4x^3a^4b^4J'-4hp_x^6a^2b^6J'\\
&-8p_x^6xa^2b^6J'-8x^7a^8A'+24p_x^2x^5a^6b^2A'\\
&-24p_x^4x^3a^4b^4A'+8p_x^6xa^2b^6A'\Big)\\
&-\epsilon^2\Big[-2hJa^2-4Jxa^2-4ha^2J'\\
&-8xa^2J'+\frac{1}{S}\Big(4h^3a^4J'+24h^2xa^4J'\\
&+48hx^2a^4J'+32x^3a^4J'+16hp_x^2a^2b^2J'\\
&+32p_x^2xa^2b^2J'\Big)+\frac{1}{S^2}\Big(-12h^3x^2a^6J'\\
&-48h^2x^3a^6J'-60hx^4a^6J'-24x^5a^6J'\\
&-4h^3p_x^2a^4b^2J'-32h^2p_x^2xa^4b^2J'\\
&-72hp_x^2x^2a^4b^2J'-48p_x^2x^3a^4b^2J'\\
&-12hp_x^4a^2b^4J'-24p_x^4xa^2b^4J'\Big)\Big]\\
&-\epsilon^4\Big[\frac{1}{2}h^3Ja^4+3h^2Jxa^4+6hJx^2a^4\\
&+4Jx^3a^4-Dh^2p_xa^3b-2Dhp_xa^3b\\
&+2hJp_x^2a^2b^2+4Jp_x^2xa^2b^2+h^3a^4J'\\
&-2h^2xa^4J'-12hx^2a^4J'-8x^3a^4J'\\
&-4hp_x^2a^2b^2J'-8p_x^2xa^2b^2J'\\
&+\frac{1}{S}\Big(-h^5a^6J'-10h^4xa^6J'-36h^3x^2a^6J'\\
&-64h^2x^3a^6J'-60hx^4a^6J'-24x^5a^6J'\\
&-8h^3p_x^2a^4b^2J'-40h^2p_x^2xa^4b^2J'\\
&+72hp_x^2x^2a^4b^2J'-48p_x^2x^3a^4b^2J'\\
&-12hp_x^4a^2b^4J'-24p_x^4xa^2b^4J'\Big)\\
&+\frac{1}{S^2}\Big(3h^5x^2a^8J'+20h^4x^3a^8J'\\
&+55h^3x^4a^8J'+78h^2x^5a^8J'\\
&+56hx^6a^8J'+16x^7a^8J'+h^5p_x^2a^6b^2J'\\
&+12h^4p_x^2xa^6b^2J'+54h^3p_x^2x^2a^6b^2J'\\
&+116h^2p_x^2x^3a^6b^2J'+120hp_x^2x^4a^6b^2J'\\
&+48p_x^2x^5a^6b^2J'+7h^3p_x^4a^4b^4J'\\
&+38h^2p_x^4xa^4b^4J'+72hp_x^4x^2a^4b^4J'\\
&+48p_x^4x^3a^4b^4J'+8hp_x^6a^2b^6J'\\
&+16p_x^6xa^2b^6J'\Big)\Big]. \qquad (16)
\end{aligned}
$$

References

[1] M Lakshmanan and S Rajasekar, *Nonlinear dynamics: Integrability, chaos and patterns* (Springer, New Delhi, 2003)
[2] F C Moon, *Nonlinear dynamics and chaos in material processing* (John Wiley and Sons, New York, 1998)
[3] L Xiao-Gang, L Wen-Jun and L Ming, *Pramana – J. Phys.* **86**, 575 (2016)
[4] E A Harris and J Owen, *Phys. Rev. Lett.* **11**, 9 (1963)
[5] D S Rodbell, I S Jacobs, J Owen and E A Harris, *Phys. Rev. Lett.* **11**, 10 (1963)
[6] D S Rodbell and J Owen, *J. Appl. Phys.* **35**, 1002 (1964)
[7] R J Birgeneau, M T Hutchings, J M Baker and J D Riley, *J. Appl. Phys.* **40**, 1070 (1969)
[8] H H Chen and P M Levy, *Phys. Rev. B* **7**, 4267 (1973)
[9] B M Matveev, *ZhETF* **65**, 1626 (1973)
[10] R Myrzakulov, M Daniel and R Amuda, *Physica A* **234**, 715 (1997)
[11] M Daniel and L Kavitha, *Phys. Rev. B* **66**, 184433 (2002)
[12] Z P Shi, G X Huang and R Tao, *Phys. Rev. B* **42**, 747 (1990)
[13] C N Kumar and A Khare, *J. Phys. A* **22**, L849 (1989)
[14] B S Gnana Blessy and M M Latha, *Physica B* **523**, 114 (2017)
[15] D N Aristov and S V Maleyev, *Phys. Rev. B* **62**, R751 (2000)
[16] I Dzyaloshinsky, *J. Phys. Chem. Solids* **4**, 241 (1958)
[17] T Moriya, *Phys. Rev.* **120**, 91 (1960)
[18] M Daniel and R Amutha, *J. Phys. A* **28**, 5529 (1995)
[19] M Daniel and R Amutha, *Phys. Rev. B* **53**, R2930 (1996)
[20] M Daniel and L Kavitha, *Phys. Rev. B* **63**, 172302 (2001)
[21] M Daniel and L Kavitha, *Phys. Lett. A* **295**, 121 (2002)
[22] R Pandit, C Tannous and J A Krumhansl, *Phys. Rev. B* **28**, 289 (1983)
[23] M E Gouvea and A S T Pires, *Phys. Rev. B* **34**, 306 (1986)
[24] S Takeno and K Kawasaki, *Phys. Rev. B* **45**, 5083 (1992)
[25] W M Liu and B L Zhou, *Phys. Lett. A* **184**, 487 (1994)
[26] R Lai, S A Kiselev and A J Sievers, *Phys. Rev. B* **54**, R12665 (1996)
[27] U T Schwarz, L Q English and A J Sievers, *Phys. Rev. Lett.* **83**, 223 (1999)
[28] L Q English, M Sato and A J Sievers, *J. Appl. Phys.* **89**, 6707 (2001)

[29] D Lissouck and J P Nguenang, *J. Phys.: Condens. Matter* **19**, 096202 (2007)
[30] J-P Nguenang, M Peyrard, A J Kenfack and T C Kofane, *J. Phys.: Condens. Matter* **17**, 3083 (2005)
[31] G X Huang, Z P Shi, X X Dai and R Tao, *J. Phys.: Condens. Matter* **2**, 10059 (1990)
[32] T Holstein and H Primakoff, *Phys. Rev.* **58**, 1098 (1940)
[33] R Ferrer, *Physica B* **56**, 132 (1985)